

# NMR Evidence of Antiferromagnetic Spin Fluctuations in $\text{Nd}_{0.85}\text{Sr}_{0.15}\text{NiO}_2$

Yi Cui,<sup>1,\*</sup> C. Li,<sup>1,\*</sup> Q. Li,<sup>2,\*</sup> Xiyu Zhu,<sup>2</sup> Z. Hu,<sup>1</sup> Yi-feng Yang,<sup>3</sup>  
J. S. Zhang,<sup>4</sup> Rong Yu,<sup>1,†</sup> Hai-Hu Wen,<sup>2,‡</sup> and Weiqiang Yu<sup>1,§</sup>

<sup>1</sup>*Department of Physics and Beijing Key Laboratory of Opto-electronic Functional Materials & Micro-nano Devices, Renmin University of China, Beijing, 100872, China*

<sup>2</sup>*National Laboratory of Solid State Microstructures and Department of Physics, Center for Superconducting Physics and Materials,*

*Collaborative Innovation Center for Advanced Microstructures, Nanjing University, Nanjing 210093, China*

<sup>3</sup>*Beijing National Laboratory for Condensed Matter Physics and Institute of Physics, Chinese Academy of Sciences, Beijing 100190, China*

<sup>4</sup>*Mathematics and Physics Department, North China Electric Power University, Beijing 102206, China*

Despite the recent discovery of superconductivity in  $\text{Nd}_{1-x}\text{Sr}_x\text{NiO}_2$  thin films, the absence of superconductivity and antiferromagnetism in their bulk materials remain a puzzle. Here we report the  $^1\text{H}$  NMR measurements on powdered  $\text{Nd}_{0.85}\text{Sr}_{0.15}\text{NiO}_2$  samples by taking advantage of the enriched proton concentration after hydrogen annealing. We find a large full width at half maximum of the spectrum, which keeps increasing with decreasing the temperature and exhibits an upturn behavior at low temperatures. The spin-lattice relaxation rate  $1/T_1$  is strongly enhanced when lowering the temperature, developing a broad peak at about 40 K, then decreases following a spin-wave-like behavior  $1/T_1 \sim T^2$  at lower temperatures. These results evidence a short-range glassy antiferromagnetic ordering of magnetic moments below 40 K and dominant antiferromagnetic fluctuations extending to much higher temperatures. Our findings reveal the strong electron correlations in bulk  $\text{Nd}_{0.85}\text{Sr}_{0.15}\text{NiO}_2$ , and shed light on the mechanism of superconductivity observed in films of nickelates.

The recent discovery of superconductivity in films of the infinite layer nickelate  $\text{Nd}_{1-x}\text{Sr}_x\text{NiO}_2$  [1, 2] with a maximal transition temperature  $T_c$  of 14.9 K has attracted a lot of research attention.  $\text{Nd}_{1-x}\text{Sr}_x\text{NiO}_2$  has the same lattice structure as the infinite-layer cuprate superconductor  $(\text{Sr}_{1-x}\text{Ca}_x)_{1-y}\text{CuO}_2$  [3]. In the undoped  $\text{NdNiO}_2$ , the  $\text{Ni}^{1+}$  ion has an electron configuration of  $3d^9$  with a single hole in the  $d_{x^2-y^2}$  orbital, as  $\text{Cu}^{2+}$  in cuprate superconductors. It was proposed that upon  $\text{Sr}^{2+}$  substitution for  $\text{Nd}^{3+}$  the nickelate behaves as a doped Mott insulator, in analogy to the hole-doped cuprates [4]. However, a number of major differences between these two systems have been noted. The charge transfer gap between the Ni  $3d$  to O  $2p$  orbitals was estimated to be much larger than that in cuprates [5, 6]. So it is under debate whether the hole introduced by Sr doping would reside on the O site as in cuprates [7], or on the Ni site forming a  $3d^8$  configuration. The latter could cause an  $S = 1$  high-spin configuration of Ni that involves multi-orbital physics [5, 8–13]. Moreover, the larger charge transfer gap leads to a smaller exchange energy [14, 15], which may substantially suppress the antiferromagnetism in the nickelate. The  $5d$  [16, 17] and  $4f$  [18] electrons in  $\text{Nd}^{3+}$ , and/or interstitial  $s$  electrons [19] may also participate to the low-energy electronic structure.

The above concerns make an open question in relation to the doped Mott insulator scenario of the nickelate and stimulates alternative theoretical proposals involving Kondo effect [11, 12], anti-Kondo effect [18], multi-orbital effect [20–22], Hund’s coupling [23], and disorder effect. Surprisingly, more recent measurements on the bulk materials show an absence of superconductivity [24] and no

long-range order antiferromagnetism [25–27]. These results not only challenge the similarity between nickelates and cuprates, but also raise an intriguing question: what could be the critical ingredients manipulating the superconductivity in film and bulk nickelates.

Both the  $\text{Nd}_{1-x}\text{Sr}_x\text{NiO}_2$  films and the powdered bulk crystals are made from  $\text{Nd}_{1-x}\text{Sr}_x\text{NiO}_3$  by post annealing in hydrogen atmosphere to remove the apical oxygen in the lattice [2, 24–26]. However, the resistivity of the powdered bulk crystals show an insulating behavior from room temperature down to 1.5 K. One may wonder the role of hydrogen annealing: besides removing the apical oxygens, could it be a key factor of tuning the superconductivity by introducing effective charge doping or inhomogeneity?

Experimental studies on the electronic structure and magnetism are much demanded to address the above questions and to get a convergent understanding of the superconductivity in general [28–31]. NMR is an ideal probe of low-energy physics in condensed matter systems, and the hydrogen annealing motivates us to search for  $^1\text{H}$  NMR in bulk  $\text{Nd}_{0.85}\text{Sr}_{0.15}\text{NiO}_2$  samples, whose film counterpart is near optimal doping [2].

In this paper, we show that the  $^1\text{H}$  NMR intensity of  $\text{Nd}_{0.85}\text{Sr}_{0.15}\text{NiO}_2$  is much larger than that of  $\text{Nd}_{0.85}\text{Sr}_{0.15}\text{NiO}_3$ , which implies a higher concentration of hydrogen after annealing. More strikingly, although the hyperfine shift  $^1K_s$  in the annealed sample is very small, a large increase of full width at half maximum (FWHM) of the spectrum is observed in  $\text{Nd}_{0.85}\text{Sr}_{0.15}\text{NiO}_2$ . The spin-lattice relaxation rate is very high, and is largely enhanced with decreasing the tem-

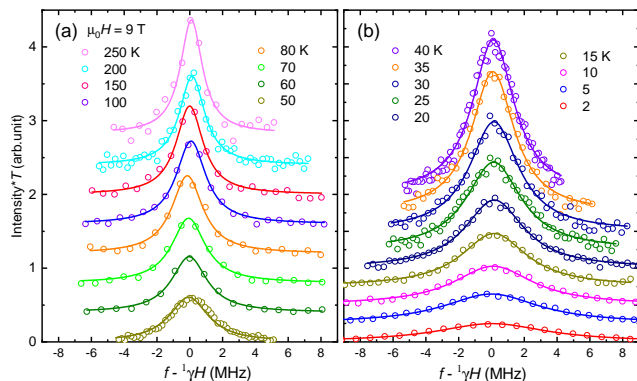


FIG. 1: The  $^1\text{H}$  NMR spectra (open circles) of  $\text{Nd}_{0.85}\text{Sr}_{0.15}\text{NiO}_2$  at a fixed field of  $\mu_0 H = 9$  T, obtained by frequency sweep at selected temperatures. The NMR intensity is obtained from the integration of the spin-echo spectrum multiplying by the temperature. For clarity, vertical shifts are applied to data at different temperatures, and vertical scales in panels (a) and (b) are chosen differently. The solid lines are function fits to the spectra with the single-Lorentzian form.

perature, developing a broad peak at about 40 K. These results signal dominant antiferromagnetic (AFM) fluctuations in the system. Below 40 K, the FWHM of the spectrum increases dramatically with an upturn behavior, and the  $1/T_1 \sim T^2$  showing a spin-wave-like behavior. These suggest a short-range or glassy AFM order developing below 40 K. The observed enhanced AFM fluctuations and the short-range AFM ordering are inherent in the strong electron correlations in the bulk materials, and are crucial for the understanding of the magnetism and superconductivity in nickelates.

The powdered samples of  $\text{Nd}_{0.85}\text{Sr}_{0.15}\text{NiO}_2$  in this study are made by the topotactic hydrogen annealing method as reported in earlier papers [24, 32]. The magnetization data are measured by a VSM in a Quantum Design PPMS (physical property measurement system). In principle it is hard to perform NMR measurements on  $\text{Nd}_{0.85}\text{Sr}_{0.15}\text{NiO}_2$  without isotope enrichment. But after annealing, hydrogen can be injected to the system given its small size. Taking this advantage,  $^1\text{H}$  (spin-1/2,  $\gamma = 42.5759$  MHz/T) NMR signal is found by using a standard spin-echo pulse sequence  $\pi/2-\tau-\pi$ , where  $\pi/2$  and  $\pi$  pulse lengths are  $1.5 \mu\text{s}$  and  $3.0 \mu\text{s}$ , respectively, and  $\tau \sim 1 \mu\text{s}$  is the blank time between two pulses. Such short pulses and  $\tau$  are selected to minimize the  $^1T_2$  effect which is found to be about  $20 \mu\text{s}$  at low temperatures. The full NMR spectrum is obtained by frequency sweep at a fixed field. The spin-lattice relaxation rate  $^1T_1$  is measured by the inversion-recovery method, and the spin-recovery is fitted by stretched exponential functions, with a stretching factor  $\beta \sim 0.7$  at temperature above 50 K and is reduced to about 0.3 when cooled down to 5 K, indicating either magnetic anisotropy or sample inhomogeneity. In addition to this short  $^1T_1$  NMR signal,

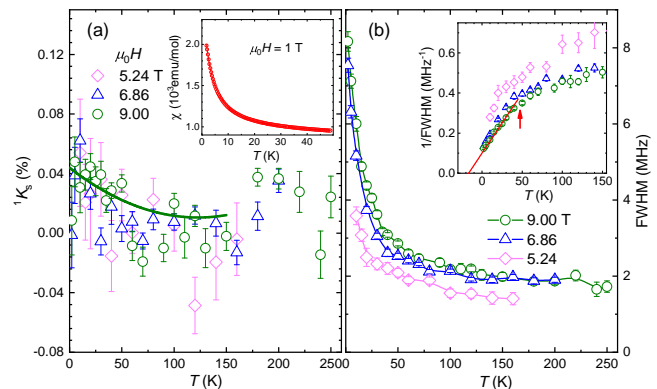


FIG. 2: (a) The NMR hyperfine shift of  $\text{Nd}_{0.85}\text{Sr}_{0.15}\text{NiO}_2$  as functions of temperatures at different fields. The solid line is a polynomial fit to the 9 T data below 150 K. Inset: The susceptibility as a function of temperature with a fixed field  $\mu_0 H = 1$  T. (b) The FWHM of the spectra of  $\text{Nd}_{0.85}\text{Sr}_{0.15}\text{NiO}_2$  as functions of temperatures. Inset: The inverse of the FWHM, which exhibits a downturn at 40 K marked by the up arrow and a linear temperature dependence below 40 K as shown by the straight line.

a long  $^1T_1$  component with a narrow bandwidth (about 100 kHz) is also found, and does not vary with sample, which should be from the environment. Considering the single-Lorentzian lineshape, we believe that the spectra in Fig. 1 represent the majority phase of the sample, instead of an impurity phase.

The  $^1\text{H}$  NMR spectra measured by frequency sweep under a constant field 9 T and various temperatures are shown in Fig. 1, where zero frequency corresponds to zero Knight shift. Upon cooling, the NMR spectra follow the Lorentzian form and barely shift with temperature. The hyperfine shift  $K_s$  (defined as  $K_s = f_p/\gamma H - 1$ , where  $f_p$  is the peak frequency of the spectrum) and the FWHM are then calculated from the spectra. Their temperature evolutions at several fields are shown in Fig. 2(a) and Fig. 2(b), respectively.  $K_s$  is very small, with a typical value less than 0.1%. Yet a weak upturn upon cooling is still resolved, which is consistent with the increase of the measured bulk susceptibility data (inset of Fig. 2(a)). The small  $K_s$  values and the upturn behavior barely depend on the field. On the other hand, as shown in Fig. 2(b) the FWHM is much larger than the hyperfine shift (relative to the zero frequency), as shown in Fig. 1, and increases with decreasing temperature from 250 K to 40 K, indicating a large magnetic broadening of the spectra.

Below 40 K, the FWHM increases rapidly with decreasing the temperature and follows an upturn behavior, as also shown by a kinked downturn (marked by the up arrow) in the inverse of the FWHM (Fig. 2(b) inset). Such a large broadening is a typical character of inhomogeneous NMR linewidth, as is much bigger than the measured  $1/T_2$  ( $T_2 \approx 20 \mu\text{s}$  at low temperatures). This large

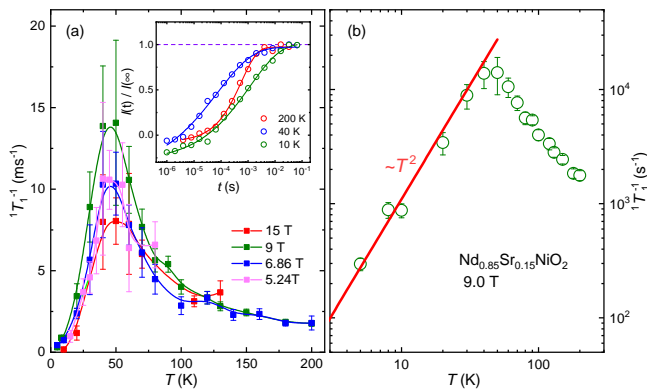


FIG. 3: (a) Measured  $1/T_1$  with temperature of  $\text{Nd}_{0.85}\text{Sr}_{0.15}\text{NiO}_2$  under different fields. Inset: The spin recovery data at three typical temperatures, and the solid lines are fits by the stretched exponential functions to obtain the  $T_1$ . (b) The low-temperature  $1/T_1$  plotted in a log-log scale. The solid line is a function fit to  $1/T_1 \sim T^{-2}$ .

linewidth and the upturn behavior are observed over a broad field range. Though the powdered sample is chemically and structurally inhomogeneous, the strong temperature dependence of the FWHM below 40 K at large fields can only be attributed to a precursor to static AFM ordering, because in an antiferromagnet, the projection of local hyperfine fields along the external field is also randomly distributed between negative and positive values when the crystalline orientations are random in powders. This is further discussed below.

The spin-lattice relaxation rate  $1/T_1$ , defined as,  $1/T_1 = T \lim_{\omega \rightarrow 0} \sum_q A_{\text{hf}}(q) \text{Im}\chi(q, \omega)/\omega$ , where  $\chi(q, \omega)$  is the dynamical susceptibility and  $A_{\text{hf}}(q)$  the hyperfine coupling, is a sensitive probe of low-energy spin fluctuations [33]. Since  $^1\text{H}$  nuclear spin is  $1/2$ , the spin-lattice relaxation rate  $1/T_1$  of  $^1\text{H}$  is only sensitive to magnetic fluctuations. The  $1/T_1$  is then measured and plotted as functions of temperatures under various fields in Fig. 3. Upon warming from 2 K, the  $1/T_1$  first increases dramatically, then forms a peaked feature at  $T \approx 40$  K, and finally flattens out at temperatures above 100 K. This peaked behavior is demonstrated by the spin-recovery curve for the  $T_1$ , as shown in the inset of Fig. 3(a), where the spin recovers more rapidly at 40 K than that at 200 K and 10 K.

A sharp peak in  $1/T_1$  is usually a signature of magnetic phase transition. Although the magnetization data revealed a spurious ferromagnetic phase in both  $\text{Nd}_{0.85}\text{Sr}_{0.15}\text{NiO}_2$  [24] and  $\text{Nd}_4\text{Ni}_3\text{O}_8$  [32, 34], its high onset temperature (above 300 K) is incompatible with our observation. Since no additional magnetic hysteresis emergent at 40 K by any other probes [24], the magnetic transition has to be an AFM type.

The broad peak at about 40 K in bulk  $\text{Nd}_{0.85}\text{Sr}_{0.15}\text{NiO}_2$  suggests the onset of glassy anti-

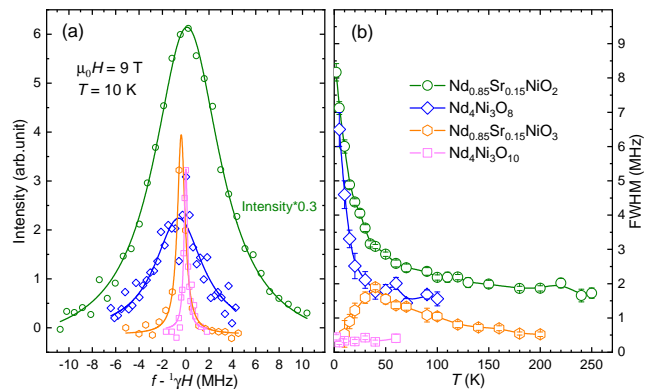


FIG. 4: (a) The  $^1\text{H}$  spectra under a field of 9 T measured on four compounds of nickelates. The spectra are measured under identical condition, such as the same sample mass, coil, NMR pulse sequences, *etc.*. Solid lines are Lorentzian-form fit to the data. (b) Corresponding FWHM as functions of temperatures, obtained by the Lorentzian-form fit to the spectra.

magnetic order, where the transition temperature varies across the sample due to inhomogeneity. This glassy behavior is similar to underdoped cuprate superconductor [35]. Nevertheless, it indicates the onset of low-energy spin fluctuations at 40 K. Below 40 K,  $1/T_1 \sim T^\alpha$ , follows a power-law behavior with a low power-law exponent  $\alpha = 2$ , much smaller than that caused by AFM spin wave excitations ( $\alpha = 5$ ) [36], again evidences remaining spin excitations. These results, together with the broad peak in  $1/T_1$  at 40 K and the large FWHM below 40 K, are fully consistent with a glassy AFM order caused by inhomogeneity at low temperatures.

In order to understand the effects of hydrogen annealing and the origin of the  $^1\text{H}$  signal, we performed comparative studies on four bulk nickelate compounds.  $\text{Nd}_{0.85}\text{Sr}_{0.15}\text{NiO}_3$  [37] and  $\text{Nd}_4\text{Ni}_3\text{O}_8$  [32] are made without hydrogen annealing, and  $\text{Nd}_{0.85}\text{Sr}_{0.15}\text{NiO}_2$  and  $\text{Nd}_4\text{Ni}_3\text{O}_8$  are synthesized after hydrogen annealing from the former two compounds [32, 38], respectively. Although  $\text{NdNiO}_3$  is insulating and antiferromagnetically ordered below 200 K [39–42],  $\text{Nd}_{0.85}\text{Sr}_{0.15}\text{NiO}_3$  shows a metallic behavior at low temperatures [37].  $\text{Nd}_4\text{Ni}_3\text{O}_{10}$  is also metallic at low temperatures [32, 34, 43], but  $\text{Nd}_4\text{Ni}_3\text{O}_8$  [32] shows an insulating behavior at low temperatures and its magnetic properties remain unknown.

The spectra of the four compounds at a representative field 9 T are shown in Fig. 4(a). Interestingly, clear  $^1\text{H}$  signals are resolved for the two samples without hydrogen annealing. This is not too surprising because hydrogen is hard to avoid in materials, given its small atomic size. However, the total integrated spectral weight of  $^1\text{H}$  in  $\text{Nd}_{0.85}\text{Sr}_{0.15}\text{NiO}_2$  is enhanced by a factor of  $\sim 45$  compared with  $\text{Nd}_{0.85}\text{Sr}_{0.15}\text{NiO}_3$ , which suggests much higher hydrogen concentration in the annealed sample. However, by comparing to some organic materials, the

concentration of hydrogen in  $\text{Nd}_{0.85}\text{Sr}_{0.15}\text{NiO}_2$  is estimated to be less than 1%. Though largely enhanced after annealing, the level of hydrogen concentration remains small and can not provide an effective carrier doping. We also tried proton injection by using the ionic liquid method [44–46], but no additional effect was observed, implying a similar hydrogen concentration. On the other hand, the measured NMR spin-lattice relaxation rate takes a typical value about  $1000 \text{ s}^{-1}$  for temperatures between 10 K and 200 K, which is much larger than that of the environmental protons, indicating that the hydrogen ions strongly couple to the magnetic moment in the sample. Therefore, instead of providing effective doping, hydrogen entered in the system serves as a sensitive local probe for the magnetic properties of the system.

The respective FWHM of the  $^1\text{H}$  NMR spectra of four compounds are shown in Fig. 4(b). For the annealed compounds, the FWHM are very large. For example, in  $\text{Nd}_{0.85}\text{Sr}_{0.15}\text{NiO}_2$  the FWHM above 50 K corresponds to 0.5% of the resonance frequency, which is over twenty times of the hyperfine shift ( $\sim 0.02\%$ ). The FWHM of  $\text{Nd}_{0.85}\text{Sr}_{0.15}\text{NiO}_2$  and  $\text{Nd}_4\text{Ni}_3\text{O}_8$  are much larger than those of unannealed samples. In particular, the FWHM in  $\text{Nd}_4\text{Ni}_3\text{O}_8$  shows a large upturn below 40 K, similar to  $\text{Nd}_{0.85}\text{Sr}_{0.15}\text{NiO}_2$ . The larger FWHM reflects stronger inhomogeneity of the annealed compounds. The origin of the inhomogeneity is two-fold. On one hand, during annealing, the removal of apical oxygen may be incomplete, and the hydrogen and Ni ions may even form Ni-H bond [47]. These can certainly increase the level of inhomogeneity in the system. Inhomogeneity promotes the localization of electrons, which explains the observed insulating behavior up to room temperature in the annealed samples. On the other hand, the prominent upturn of FWHM below 40 K in the annealed samples should be associated with magnetic fluctuations, because at low temperatures the charge and structural inhomogeneities are quenched and can not account for such a strong temperature dependence.

In the following, we discuss the nature of the observed AFM fluctuations in bulk  $\text{Nd}_{0.85}\text{Sr}_{0.15}\text{NiO}_2$ . At present, we cannot differentiate whether the magnetic fluctuations are caused by Nd or Ni moments. Nonetheless, the Nd magnetic ordering can be induced by the Ni magnetic ordering through their couplings [42, 48]. In either case, our result indicates the existence of intrinsic order of Ni moments. Consider the dipolar hyperfine coupling between one Ni/Nd moment and the neighbouring  $^1\text{H}$  nuclei (assuming in the apical positions), the FWHM of 4 MHz at 5.24 T gives an estimation of magnetic moment about  $0.2 \mu_B$ , which is near the limit of resolution of neutron diffraction and may not be observed [25–27]. The broad peak of  $1/T_1$  at around 40 K indicates the strength of magnetic couplings is at the order of 10 meV. Indeed, the super-exchange coupling among nearest Ni moments

is estimated theoretically to be 10-30 meV [5, 6, 14, 15], consistent with our observations.

Our results support the existence of antiferromagnetically interacting Ni moments and are consistent with the doped Mott insulator scenario of nickelates. The onset of short-range ordering at 40 K coincides with the upturn of the low-temperature resistivity [24], which suggests an enhanced insulating behavior through magnetic scattering, as seen in quasi-1D Bechgaard salts [49]. A recent RIXS measurement suggests the doped hole results in a low-spin state of the Ni  $3d^8$  configuration [50], which is also consistent with this picture. Nonetheless, the alternative picture, in which the doped hole leads to a high-spin  $3d^8$  Ni configuration [23, 51], cannot be differentiated from our current data. Measurements on how the AFM fluctuations and short-range order evolve with different rare earth and/or hole doping would tell more information on whether a low-spin or a high-spin configuration is favored. As an interesting proposal, the  $\text{Ni}^{+1}$  moments could hybridize with Nd  $5d$  itinerant electrons to form Kondo singlets [11]. In  $\text{Nd}_{0.85}\text{Sr}_{0.15}\text{NiO}_2$ , we do not observe an effect of Kondo-singlet formation which would cause a constant  $1/T_1T$  at low temperatures [52]. A likely picture could be the Nd  $5d$  bands are already emptied by the hole doping of  $\text{Sr}^{2+}$  at  $x = 0.15$ , and the Kondo effect would be more relevant in the underdoped regime. Interestingly, the FWHM with temperature of  $\text{Nd}_{0.85}\text{Sr}_{0.15}\text{NiO}_3$  shows a peak at about 40 K and drops rapidly at low temperatures (Fig. 4(b)). Whether the Kondo physics is relevant there deserves further study.

Finally, we discuss the implication to superconductivity of the nickelate. The observation of AFM fluctuations and short-range magnetic ordering in the bulk materials suggests that the superconductivity in the nickelate is mediated via spin fluctuations, analogous to cuprate and iron-based superconductors. In the bulk materials, the absence of superconductivity and long-range antiferromagnetism would imply strong competition between several ordered phases, while the strong inhomogeneity in the system prevents formation of any long-range order. As for the films, similar AFM fluctuations are expected, from which superconductivity emerges. However, some factors could be unique to the films. First, with typical thickness of  $\sim 10 \text{ nm}$  [1, 2], it should be easier to achieve oxygen homogeneity upon annealing, and a more homogeneous environment helps acquiring the phase coherence for superconductivity. Indeed, in superconducting  $\text{Nd}_{0.8}\text{Sr}_{0.2}\text{NiO}_2$  films the resistivity remains metallic up to room temperature [2], indicating a much higher level of electron homogeneity. Furthermore, the  $\text{SrTiO}_3$  substrate may provide additional doping or other interfacial effects to suppress the static AFM order and induce superconductivity in thin films. An example of the interface enhanced superconductivity has been realized in the single-layer FeSe film grown on the  $\text{SrTiO}_3$  substrates [53, 54].

To summarize, we have performed  $^1\text{H}$  NMR measurements on the hydrogen-annealed powdered  $\text{Nd}_{0.85}\text{Sr}_{0.15}\text{NiO}_2$  samples, and observed enhanced AFM fluctuations below 100 K and emergence of a short-range AFM order below 40 K. These properties are inherent to the strong correlations of Ni magnetic moments in  $\text{Nd}_{0.85}\text{Sr}_{0.15}\text{NiO}_2$ . Although superconductivity and long-range AFM order are not observed, likely due to the high inhomogeneity after annealing, the finding of strong AFM fluctuations pave the way for the understanding of superconductivity in nickelates.

This work is supported by the National Natural Science Foundation of China with Grant Nos. 51872328, 11674392, 11774401 and A0402/11927809, the Ministry of Science and Technology of China with Grant Nos. 2016YFA0300504 and 2016YFA0300401, China Postdoctoral Science Foundation with Grant No. 2020M680797, the Fundamental Research Funds for the Central Universities, and the Research Funds of Renmin University of China with Grant Nos. 18XNLG24, 20XNLG19 and 21XNLG18.

\* These authors contributed equally to this study.

† Electronic address: [rong.yu@ruc.edu.cn](mailto:rong.yu@ruc.edu.cn)

‡ Electronic address: [hhwen@nju.edu.cn](mailto:hhwen@nju.edu.cn)

§ Electronic address: [wqyu\\_phy@ruc.edu.cn](mailto:wqyu_phy@ruc.edu.cn)

- [1] D. Li, K. Lee, B. Wang, M. Osada, S. Crossley, H. R. Lee, Y. Cui, Y. Hikita, and H. Y. Hwang, *Superconductivity in an infinite-layer nickelate*, **Nature** **572**, 624 (2019).
- [2] D. Li, B. Wang, K. Lee, S. P. Harvey, M. Osada, B. H. Goodge, L. F. Kourkoutis, and H. Y. Hwang, *Superconducting Dome in  $\text{Nd}_{1-x}\text{Sr}_x\text{NiO}_2$  Infinite Layer Films*, **Phys. Rev. Lett.** **125**, 027001 (2020).
- [3] M. Azuma, Z. Hiroi, M. Takano, Y. Bando, and Y. Takeda, *Superconductivity at 110 K in the infinite-layer compound  $(\text{Sr}_{1-x}\text{Ca}_x)_{1-y}\text{CuO}_2$* , **Nature** **356**, 775 (1992).
- [4] V. I. Anisimov, D. Bukhvalov, and T. M. Rice, *Electronic structure of possible nickelate analogs to the cuprates*, **Phys. Rev. B** **59**, 7901 (1999).
- [5] A. S. Botana and M. R. Norman, *Similarities and Differences between  $\text{LaNiO}_2$  and  $\text{CaCuO}_2$  and Implications for Superconductivity*, **Phys. Rev. X** **10**, 011024 (2020).
- [6] A. Fujimori, *Electronic structure, magnetism, and superconductivity in infinite-layer nickelates*, **Journal Club for Condensed Matter Physics** **10.36471** (2019).
- [7] Z.-J. Liang, R. Jiang, and W. Ku, *Where do the doped hole carriers reside in the new superconducting nickelates?* [arXiv:2005.00022](https://arxiv.org/abs/2005.00022) (2020).
- [8] Michael R. Norman, *Entering the Nickel Age of Superconductivity*, **Physics** **13**, 85 (2020).
- [9] S. Ryee, H. Yoon, T. J. Kim, M. Y. Jeong, and M. J. Han, *Induced magnetic two-dimensionality by hole doping in the superconducting infinite-layer nickelate  $\text{Nd}_{1-x}\text{Sr}_x\text{NiO}_2$* , **Phys. Rev. B** **101**, 064513 (2020).
- [10] X. Wu, D. D. Sante, T. Schwemmer, W. Hanke, H. Y. Hwang, S. Raghu, and R. Thomale, *Robust  $d_{x^2-y^2}$ -wave superconductivity of infinite-layer nickelates*, **Phys. Rev. B** **101**, 060504(R) (2020).
- [11] G.-M. Zhang, Y.-F. Yang, and F.-C. Zhang, *Self-doped Mott insulator for parent compounds of nickelate superconductors*, **Phys. Rev. B** **101**, 020501(R) (2020).
- [12] B. H. Goodge, D. Li, K. Lee, M. Osada, B. Y. Wang, G. A. Sawatzky, H. Y. Hwang, and L. F. Kourkoutis, *Doping evolution of the Mott-Hubbard landscape in infinite-layer nickelates*, **Proc. Natl. Acad. Sci. USA** **12**, 118 (2020).
- [13] J. Karp, A. Hampe, M. Zing, A. S. Botana, H. Park, M. R. Norman, and A. J. Millis, *Comparative Many-Body Study of  $\text{Pr}_4\text{Ni}_3\text{O}_8$  and  $\text{NdNiO}_2$* , **Phys. Rev. B** **102**, 245130 (2020).
- [14] M. Jiang, M. Berciu, and G. A. Sawatzky, *Critical Nature of the Ni Spin State in Doped  $\text{NdNiO}_2$* , **Phys. Rev. Lett.** **124**, 207004 (2020).
- [15] A. E. Bocquet, T. Mizokawa, K. Morikawa, A. Fujimori, S. R. Barman, K. Maiti, D. D. Sarma, Y. Tokura, and M. Onoda, *Electronic structure of early 3d-transition-metal oxides by analysis of the 2p core-level photoemission spectra*, **Phys. Rev. B** **53**, 1161 (1996).
- [16] M. Hepting, D. Li, C. J. Jia, H. Lu, E. Paris, Y. Tseng, X. Feng, M. Osada, E. Been, Y. Hikita, Y.-D. Chuang, Z. Hussain, K. J. Zhou, A. Nag, M. Garcia-Fernandez, M. Rossi, H. Y. Huang, D. J. Huang, Z. X. Shen, T. Schmitt, H. Y. Hwang, B. Moritz, J. Zaanen, T. P. Devereaux, and W. S. Lee, *Electronic structure of the parent compound of superconducting infinite-layer nickelates*, **Nat. Mater.** **19**, 381 (2020).
- [17] K.-W. Lee and W. E. Pickett, *Infinite-layer  $\text{LaNiO}_2$ :  $\text{Ni}^{1+}$  is not  $\text{Cu}^{2+}$* , **Phys. Rev. B** **70**, 165109 (2004).
- [18] M.-Y. Choi, K.-W. Lee, and W. E. Pickett, *Role of 4f states in infinite-layer  $\text{NdNiO}_2$* , **Phys. Rev. B** **101**, 020503(R) (2020).
- [19] Y. Gu, S. Zhu, X. Wang, J. Hu, and H. Chen, *A substantial hybridization between correlated Ni-d orbital and itinerant electrons in infinite-layer nickelates*, **Commun. Phys.** **3**, 84 (2020).
- [20] J. Chaloupka and G. Khaliullin, *Orbital Order and Possible Superconductivity in  $\text{LaNiO}_3/\text{LaMO}_3$  Superlattices*, **Phys. Rev. Lett.** **100**, 016404 (2008).
- [21] I. Leonov, S. L. Skornyakov, and S. Y. Savrasov, *Lifshitz transition and frustration of magnetic moments in infinite-layer  $\text{NdNiO}_2$  upon hole doping*, **Phys. Rev. B** **101**, 241108(R) (2020).
- [22] P. Mandal, R. K. Patel, D. Rout, R. Banerjee, R. Bag, K. Karmakar, A. Narayan, J. W. Freeland, S. Singh, and S. Middey, *Giant orbital polarization of  $\text{Ni}^{2+}$  in a square planar environment*, **Phys. Rev. B** **103**, L060504 (2021).
- [23] Y. Wang, C.-J. Kang, H. Miao, and G. Kotliar, *Hund's metal physics: From  $\text{SrNiO}_2$  to  $\text{LaNiO}_2$* , **Phys. Rev. B** **102**, 161118(R) (2020).
- [24] Q. Li, C. He, J. Si, X. Zhu, Y. Zhang, and H.-H. Wen, *Absence of superconductivity in bulk  $\text{Nd}_{1-x}\text{Sr}_x\text{NiO}_2$* , **Commun. Mater.** **1**, 16 (2020).
- [25] M. A. Hayward, M. A. Green, M. J. Rosseinsky, and J. Sloan, *Sodium Hydride as a Powerful Reducing Agent for Topotactic Oxide Deintercalation: Synthesis and Characterization of the Nickel(I) Oxide  $\text{LaNiO}_2$* , **J. Am. Chem. Soc.** **121**, 8843 (1999).
- [26] M. A. Hayward and M. J. Rosseinsky, *Synthesis of the infinite layer Ni(I) phase  $\text{NdNiO}_{2+x}$  by low temperature reduction of  $\text{NdNiO}_3$  with sodium hydride*, **Solid State Sci.** **5**, 839 (2003).
- [27] B.-X. Wang, H. Zheng, E. Krivyakina, O. Chmaissem,

- P. P. Lopes, J. W. Lynn, L. C. Gallington, Y. Ren, S. Rosenkranz, J. F. Mitchell, and D. Phelan, *Synthesis and characterization of bulk  $Nd_{1-x}Sr_xNiO_2$  and  $Nd_{1-x}Sr_xNiO_3$* , **Phys. Rev. Materials** **4**, 084409 (2020).
- [28] Y.-T. Shao, W.-S. Hong, S.-L. Li, Z. Li, and J.-L. Luo,  *$^{19}F$  NMR Study of the Bilayer Iron-Based Superconductor  $KCa_2Fe_4As_4F_2$* , **Chin. Phys. Lett.** **36**, 127401 (2019).
- [29] Q. Wu, H. Zhou, Y. Wu, L. Hu, S. Ni, Y. Tian, F. Sun, F. Zhou, X. Dong, Z. Zhao, and J. Zhao, *Ultrafast Quasiparticle Dynamics and Electron-Phonon Coupling in  $(Li_{0.84}Fe_{0.16})OHFe_{0.98}Se$* , **Chin. Phys. Lett.** **37**, 097802 (2020).
- [30] Y.-T. Jia, C.-S. Gong, Y.-X. Liu, J.-F. Zhao, C. Dong, G.-Y. Dai, X.-D. Li, H.-C. Lei, R.-Z. Yu, G.-M. Zhang, and C.-Q. Jin, *Mott Transition and Superconductivity in Quantum Spin Liquid Candidate  $NaYbSe_2$* , **Chin. Phys. Lett.** **37**, 097404 (2020).
- [31] Z.-Y. Liu, Q.-X. Dong, P.-F. Shan, Y.-Y. Wang, J.-H. Dai, R. Jana, K.-Y. Chen, J.-P. Sun, B.-S. Wang, X.-H. Yu, G.-T. Liu, Y. Uwatoko, Y. Sui, H.-X. Yang, G.-F. Chen, and J.-G. Cheng, *Pressure-Induced Metalization and Structural Phase Transition in the quasi-One-Dimensional  $TlFeSe_2$* , **Chin. Phys. Lett.** **37**, 047102 (2020).
- [32] Q. Li, C. He, X. Zhu, J. Si, X. Fan, and H.-H. Wen, *Contrasting physical properties of the trilayer nickelates  $Nd_4Ni_3O_{10}$  and  $Nd_4Ni_3O_8$* , **Sci. China Phys. Mech. Astron.** **64**, 227411 (2021).
- [33] T. Moriya, *The effect of electron-electron interaction on the nuclear spin relaxation in metals*, **J. Phys. Soc. Jpn.** **18**, 516 (1963).
- [34] B.-Z. Li, C. Wang, P. T. Yang, J. P. Sun, Y.-B. Liu, J. Wu, Z. Ren, J.-G. Cheng, G.-M. Zhang, and G.-H. Cao, *Metal-to-metal transition and heavy-electron state in  $Nd_4Ni_3O_{10-\delta}$* , **Phys. Rev. B** **101**, 195142 (2020).
- [35] R. F. Kiefl, J. H. Brewer, J. Carolan, P. Dosanjh, W. N. Hardy, R. Kadono, J. R. Kempton, R. Krahn, P. Schleger, B. X. Yang, Hu Zhou, G. M. Luke, B. Sternlieb, Y. J. Uemura, W. J. Kossler, X. H. Yu, E. J. Ansaldo, H. Takagi, S. Uchida, and C. L. Seaman, *Muon-spin-rotation study of magnetism in  $La_{1.85}Sr_{0.15}CuO_4$  and  $YBa_2Cu_3O_x$  below 90 mK*, **Phys. Rev. Lett.** **63**, 2136 (1989).
- [36] A. Abragam, *Principles of Nuclear Magnetism* (Oxford University Press, Oxford, 1961).
- [37] J. A. Alonso, M. J. Martínez-Lope, and M. A. Hidalgo, *Hole and Electron Doping of  $RNiO_3$  ( $R=La,Nd$ )*, **J. Solid State Chem.** **116**, 146 (1995).
- [38] R. Retoux, J. Rodriguez-Carvaja, and P. Lacorre, *Neutron Diffraction and TEM Studies of the Crystal Structure and Defects of  $Nd_4Ni_3O_8$* , **J. Solid State Chem.** **140**, 307 (1998).
- [39] A. D. Caviglia, M. Först, R. Scherwitzl, V. Khanna, H. Bromberger, R. Mankowsky, R. Singla, Y.-D. Chuang, W. S. Lee, O. Krupin, W. F. Schlotter, J. J. Turner, G. L. Dakovski, M. P. Minitti, J. Robinson, V. Scagnoli, S. B. Wilkins, S. A. Cavill, M. Gibert, S. Gariglio, P. Zubko, J.-M. Triscone, J. P. Hill, S. S. Dhesi, and A. Cavalleri, *Photoinduced melting of magnetic order in the correlated electron insulator  $NdNiO_3$* , **Phys. Rev. B** **88**, 220401(R) (2013).
- [40] D. Kumar, K. P. Rajeev, J. A. Alonso, and M. J. Martínez-Lope, *Spin-canted magnetism and decoupling of charge and spin ordering in  $NdNiO_3$* , **Phys. Rev. B** **88**, 014410 (2013).
- [41] M. K. Hooda and C. S. Yadav, *Electronic properties and the nature of metal insulator transition in  $NdNiO_3$  prepared at ambient oxygen pressure*, **Physica B** **491**, 31 (2016).
- [42] V. Scagnoli, U. Staub, Y. Bodenthin, M. García-Fernández, A. M. Mulders, G. I. Meijer, and G. Hammerl, *Induced noncollinear magnetic order of  $Nd^{3+}$  in  $NdNiO_3$  observed by resonant soft x-ray diffraction*, **Phys. Rev. B** **77**, 115138 (2008).
- [43] A. Olafsen, H. Fjellvåg, and B. C. Hauback, *Crystal Structure and Properties of  $Nd_4Co_3O_{10+\delta}$  and  $Nd_4Ni_3O_{10-\delta}$* , **J. Solid State Chem.** **151**, 46 (2000).
- [44] Y. Cui, G. Zhang, H. Li, H. Lin, X. Zhu, H.-H. Wen, G. Wang, J. Sun, M. Ma, Y. Li, D. Gong, T. Xie, Y. Gu, S. Li, H. Luo, P. Yu, and W. Yu, *Protonation induced high- $T_c$  phases in iron-based superconductors evidenced by NMR and magnetization measurements*, **Sci. Bull.** **63**, 11 (2018).
- [45] Y. Cui, Z. Hu, J. Zhang, W. Ma, M. Ma, Z. Ma, C. Wang, J. Yan, J. Sun, J. Cheng, S. Jia, Y. Li, J. Wen, H. Lei, P. Yu, W. Ji, and W. Yu, *Ionic-Liquid gating induced protonation and superconductivity in  $FeSe$ ,  $FeSe_{0.93}S_{0.07}$ ,  $ZrNCl$ ,  $1T-TaS_2$  and  $Bi_2Se_3$* , **Chin. Phys. Lett.** **36**, 077401 (2019).
- [46] X. Wei, H.-B Li, Q. Zhang, D. Li, M. Qin, L. Xu, W. Hu, Q. Huan, L. Yu, J. Miao, J. Yuan, B. Zhu, A. Kusmartseva, F. V. Kusmartsev, A. V. Silhanek, T. Xiang, W. Yu, Y. Lin, L. Gu, P. Yu, Q. Chen, and K. Jin, *A selective control of volatile and non-volatile superconductivity in an insulating copper oxide via ionic liquid gating*, **Sci. Bull.** **65**, 1607 (2020).
- [47] L. Si, W. Xiao, J. Kaufmann, J. M. Tomczak, Y. Lu, Z. Zhong, and K. Held, *Topotactic Hydrogen in Nickelate Superconductors and Akin Infinite-Layer Oxides  $ABO_2$* , **Phys. Rev. Lett.** **124**, 166402 (2020).
- [48] Z. Liu, Z. Ren, W. Zhu, Z. Wang, and J. Yang, *Electronic and magnetic structure of infinite-layer  $NdNiO_2$ : trace of AFM metal*, **npj Quantum Mater.** **5**, 31 (2020).
- [49] A. G. Lebed (Ed.), *The Physics of Organic Superconductors and Conductors*, (Springer Series in Materials Science, Vol. 110, Springer, 2008).
- [50] M. Rossi, H. Lu, A. Nag, D. Li, M. Osada, K. Lee, B. Y. Wang, S. Agrestini, M. Garcia-Fernandez, Y.-D. Chuang, Z. X. Shen, H. Y. Hwang, B. Moritz, K.-J. Zhou, T. P. Devereaux, and W. S. Lee, *Orbital and spin character of doped carriers in infinite-layer nickelates*, **arXiv:2011.00595** (2020).
- [51] Y.-H. Zhang and A. Vishwanath, *Type-II  $t$ - $J$  model in superconducting nickelate  $Nd_{1-x}Sr_xNiO_2$* , **Phys. Rev. Research** **2**, 023112 (2020).
- [52] A. C. Hewson, *The Kondo Problem to Heavy Fermions*, (Cambridge University Press, 2009).
- [53] Q.-Y. Wang, Z. Li, W.-H. Zhang, Z.-C. Zhang, J.-S. Zhang, W. Li, H. Ding, Y.-B. Ou, P. Deng, K. Chang, J. Wen, C.-L. Song, K. He, J.-F. Jia, S.-H. Ji, Y.-Y. Wang, L.-L. Wang, X. Chen, X.-C. Ma, and Q.-K. Xue, *Interface-Induced High-Temperature Superconductivity in Single Unit-Cell  $FeSe$  Films on  $SrTiO_3$* , **Chin. Phys. Lett.** **29**, 037402 (2012).
- [54] Z.-X. Li, F. Wang, H. Yao, and D.-H. Lee, *What makes the  $T_c$  of monolayer  $FeSe$  on  $SrTiO_3$  so high: a sign-problem-free quantum Monte Carlo study*, **Sci. Bull.** **61**, 925 (2016).